THE FULL-SPECTRUM CORRELATED–K DISTRIBUTION AND ITS RELATIONSHIP TO THE WEIGHTED-SUM-OF-GRAY-GASES METHOD

Michael F. Modest and Hongmei Zhang
Mechanical Engineering Department
The Pennsylvania State University
University Park, PA16802
Email: mfm@mara.me.psu.edu

ABSTRACT

A new Full-Spectrum correlated–*k* distribution has been developed, which provides an efficient means for accurate radiative transfer calculations in absorbing/emitting molecular gases. The Full-Spectrum correlated–*k* distribution can be used together with any desired solution method to solve gray–medium radiative transfer equations for a small number of gray absorption coefficients, followed by numerical quadrature. It is shown that the Weighted-Sum-of-Gray-Gases model is effectively only a crude implementation of the Full-Spectrum correlated–*k* distribution approach.

Within the limits of the Full-Spectrum correlated–*k* distribution model (i.e., an absorption coefficient obeying the so-called "scaling approximation"), the method is exact. This is demonstrated by comparison with line-by-line calculations for a one-dimensional CO_2–N_2 gas mixture with varying temperature and concentration fields.

INTRODUCTION

Radiative heat transfer in gases has important applications from combustion systems to modeling atmospheric processes. The magnitude of radiative heat fluxes can have profound effects on combustion performance and environmental impact. Radiative heat transfer calculations in combustion gases may be loosely grouped into three methods (in order of decreasing complexity): (1) line-by-line calculations, (2) band models, and (3) global models.

Line-by-line calculations are the most accurate to date, but they require vast amounts of computer resources. This is undesirable even with the availability of powerful supercomputers, since radiative calculations are only a small part of a sophisticated fire/combustion code. Many studies have been devoted to narrow and wide band models, such as the Malkmus narrow band model, the correlated–*k* (CK) model and many others. The CK method is based on the fact that inside a spectral band $\Delta\eta$, which is sufficiently narrow to assume a constant Planck function, the precise knowledge of each line position is not required for the computation. In this paper the CK approach is extended to the whole spectrum by defining a Planck function weighted cumulative *k*–distribution function.

The most common global method is the so-called Weighted-Sum-of-Gray-Gases model. The concept of the WSGG approach was first presented by Hottel and Sarofim [1] within the framework of the zonal method. The method could be applied to arbitrary geometries with varying absorption coefficients, but was limited to nonscattering media confined within a black-walled enclosure. Modest [2] has shown that this model may be generalized for use with any arbitrary solution method. It was demonstrated that the total heat transfer rates can be accuratedly determined by summing solutions of the following RTEs, one for each gray gas:

$$\frac{dI_j}{ds} = \kappa_j (a_j \frac{\sigma T^4}{\pi} - I_j)$$

Here, I_j, κ_j, and a_j are the intensity, absorption coefficient, and corresponding weight associated with the j-th gray gas. Denison and Webb [3–8] have improved on the WSGG model and have developed the Spectral-Line-Based Weighted-Sum-of-Gray-Gases (SLW) model based on detailed spectral line data. They also extended the SLW model to nonisothermal and nonhomogeneous media by introducing a cumulative distribution function of the absorption coefficient, calculated over the whole spectrum and weighted by the Planck function. The absorption distribution function (ADF) approach [9–11] is almost identical to the SLW model and differs from the SLW only in the calculation of the weights a_j. These weights are chosen in such a manner that emission by an isothermal gas is rigorously predicted

for actual spectra. This method has been further generalized [10] by introducing fictitious gases (ADFFG) employing a joint distribution function that separates the κ_η into two or more fictitious gases, and is designed to be more suitable for the treatment of nonhomogeneous media.

In this paper, the Full-Spectrum correlated–*k* distribution approach is developed based on Weighted-Sum-of-Gray-Gases arguments. This approach provides a smoother — and, therefore, more easily integrated — set of weight functions than the ADF method. Through these arguments the Weighted-Sum-of-Gray-Gases model is shown to be simply a crude implementation of the FSCK (Full-Spectrum correlated–*k* distribution) developed here. Therefore, it is clear that the WSGG method, like the correlated–*k* approach, is not limited to black-walled enclosures without scattering [2], but can accomodate gray walls as well as gray scattering particles. This is also shown through direct WSGG arguments.

THEORETICAL FORMULATION

Consider an absorbing/emitting medium inside a black enclosure. We will assume here that the medium does not scatter, and that it consists primarily of molecular combustion gases (such as H_2O and CO_2 mixed in air) with their thousands of spectral lines, plus perhaps some non–scattering particles, such as soot. For such a situation the radiative equation of transfer (RTE) is given by [12]

$$\frac{dI_\eta}{ds} = \kappa_\eta (I_{b\eta} - I_\eta), \tag{1}$$

where I_η is the spectral intensity varying along a path s, η is wavenumber, $I_{b\eta}$ the Planck function, and κ_η is the spectral absorption coefficient, which (besides wavenumber) depends on local temperature, pressure and concentrations. This is our starting point to make the line-by-line calculations. The formal solution to equation (1) is [12]

$$I_\eta(s) = I_{bw\eta}\, e^{-\int_0^s \kappa_\eta ds''} + \int_0^s I_{b\eta}(T(s'))e^{-\int_{s'}^s \kappa_\eta ds''} \kappa_\eta(s')ds'. \tag{2}$$

where the subscript w denotes a value at the wall. Integrated over the entire spectrum this becomes [2]

$$I(s) = \int_0^\infty I_\eta\, d\eta = I_{bw}[1 - \alpha(T_w, 0 \to s)] - \int_0^s I_b(s')\frac{\partial \alpha}{\partial s'}(T(s'), s' \to s)ds', \tag{3}$$

where

$$\alpha(T, s' \to s) = \frac{1}{I_b(T)} \int_0^\infty I_{b\eta}(T) \left[1 - e^{-\int_{s'}^s \kappa_\eta ds''}\right] d\eta \tag{4}$$

is the total absorptivity for a gas column $s' \to s$ for irradiation from a blackbody source at temperature T. We will now assume that the commonly used "scaling approximation" applies, i.e., that spectral and spatial dependence of the absorption coefficient are separable,

$$\kappa_\eta(\eta, T, p, \text{ concentration}) = k_\eta(\eta)\, u(T, p, \text{ concentration}). \tag{5}$$

This approximation is used, for example, in the popular Curtis-Godson approximation to calculate narrowband absorptivities for non-homogeneous paths [13], and in correlated–*k* models applied to non-homogeneous atmospheres [14,15]. While a good approximation for soot, its accuracy is more limited for molecular gases: if we assume spectral lines of Lorentz shape we get [12]

$$\kappa_\eta(\eta, T, p, \text{ concentration}) = \sum_j \frac{S_j}{\pi} \frac{b_j}{(\eta - \eta_j)^2 + b_j^2}, \tag{6}$$

where η_j is the spectral position of the center of the j-th line, b_j is the line's half width at half height, and S_j is the line's intensity. In order for equation (5) to hold, we need all b_j to be constant (usually fairly true if total pressure is constant) and all S_j to have the same spatial dependence (the S_j depend only on temperature and density of the absorbing specie). Equation (5) has been shown to give very accurate results in atmospheric applications, even for strong variations in total pressure [14, 16], but—due to hot lines with strongly different temperature dependence of the line intensities—may become less accurate in the presence of fields with extreme temperature variations [17–19].

Sticking equation (5) into equations (2) and (4) yields

$$I_\eta(s) = I_{bw\eta} e^{-k_\eta X(0,s)} + \int_0^s I_{b\eta}(s') e^{-k_\eta X(s',s)} k_\eta u(s')ds', \tag{7}$$

$$\alpha(T, s' \to s) = \frac{1}{I_b(T)} \int_0^\infty I_{b\eta} \left[1 - e^{k_\eta X(s',s)}\right] d\eta. \tag{8}$$

where

$$X(s', s) = \int_{s'}^s u(s'')ds''$$

In the *k*–distribution method it is recognized that—over a small spectral interval over which $I_{b\eta}$ may be assumed constant—the absorption coefficient attains the same value many times. If the medium is homogenous [i.e., $\kappa_\eta = \kappa_\eta(\eta)$ only], and even if equation (5) applies, the absorption coefficient may be reordered into a monotonically increasing function without loss of accuracy. For the narrow spectral interval we then write for the narrowband transmissity $\overline{\tau}_\eta$

$$\overline{\tau}_\eta = \frac{1}{\Delta\eta}\int_{\Delta\eta} e^{-k_\eta X}\,d\eta = \int_0^\infty e^{-kX} f(k)dk = \int_0^1 e^{-k(g)X}\,dg, \tag{9}$$

where the cumulative *k*–distribution

$$g(k) = \int_0^k f(k)dk \tag{10}$$

is an equivalent, non-dimensional wavenumber. In equation (9) the integration can be switched from η to k_η, since for each η there is only a single value of k_η (but many different η for each k_η).

A similar argument can be applied to the entire spectrum. Defining a fractional Planck function as

$$i(T,\eta) = \frac{1}{I_b(T)}\int_0^\eta I_{b\eta}d\eta, \tag{11}$$

we can rewrite equation (8) as

$$\alpha(T, s' \rightarrow s) = 1 - \tau(T, s' \rightarrow s) = 1 - \int_0^1 e^{-k_\eta(i)X(s',s)}di. \tag{12}$$

We note there is only one value of k_η for each value of i (but many values of i for a single value of k_η). Thus, we may reorder equation (12) in the same way as equation (9), leading to

$$\tau = \int_0^1 e^{-k_\eta(i)X}di = \int_0^\infty e^{-kX} f(T,k)dk = \int_0^1 e^{-k(T,g)X}\,dg. \tag{13}$$

Here g is no longer an equivalent wavenumber, but an equivalent fractional Planck function. Note that, since i is a function of temperature so is *k*, i.e. $k = k(T,g)$. Since we would like to be able to use arbitrary methods for the solution of the radiative transfer problem, employing the simplified *k*–*g* relation of equation (13) (rather than k_η–η), the temperature dependence of $k(T,g)$ is rather inconvenient. Following Modest [2] we desire a form which upon substitution into equation (3) can be shown to reduce back to the original RTE, equation (1). We will, therefore, carry out one more reordering step to modify equation (13) to

$$\tau = \int_0^1 e^{-k(T,g)X}\,dg = \int_0^1 a(T,g_0)e^{-k(T_0,g_0)X}\,dg_0, \tag{14}$$

where $k(T_0,g_0)$ is the *k*–g distribution evaluated at a reference temperature T_0, i.e., we have moved the temperature dependence from the exponent (in *k*) to a base function a. How this is done is best understood by looking at Fig.1, which shows two typical *k*–distributions for T_0 (the reference temperature) and some other temperature T. Both functions have identical values for k=$k_{\min}$ at g=0 (the minimum absorption coefficient across the spectrum, usually zero), and k=$k_{\max}$ at g=1 (the maximum absorption coefficient across the spectrum); for each value of *k* the corresponding value for g is simply shifted. Now setting $k(T,g)$=$k(T_0,g_0)$, and differentiating leads to

$$dg = \frac{\partial k(T_0,g_0)/\partial g_0}{\partial k(T,g)/\partial g}dg_0 = \frac{f[T,k(g)]}{f[T_0,k(g_0)]}dg_0 = a(T,g_0)dg_0, \tag{15}$$

where we have arbitrarily set $a(T_0,g_0) \equiv 1$ at the reference condition.

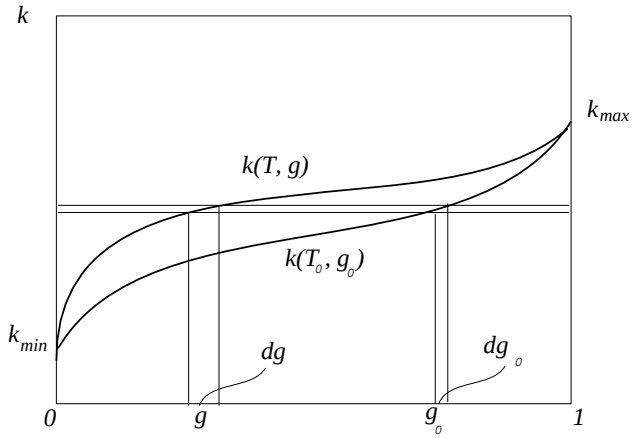

Figure 1. The weight function a, obtained from *k*–distributions at different temperatures

For simplicity of notation we will, from now on, drop the subscript 0 from g_0, as well as the argument T_0 from $k(T_0,g_0)$, which then is simply written as $k(g)$. Substituting equation (14) into equation (3), and noting that

$$\frac{\partial\alpha}{\partial s'} = -\frac{\partial\tau}{\partial s'} = \int_0^1 a(T,g)e^{-k(g)X(s',s)}k(g)\frac{\partial X}{\partial s'}dg$$

$$= - \int_0^1 a(T, g) e^{-k(g)X} k(g) u(s') \, dg$$

we obtain

$$I(s) = I_{bw} \int_0^1 a\,(T_w, g) e^{-kX(0,s)} dg + \int_0^s I_b(s') \int_0^1 a\,[T(s'), g] e^{-k(g)X(s',s)} k(g) u(s') dg \, ds' \quad (16)$$

If we now introduce a new "spectral" intensity $I_g\,(s)$, we get

$$I(s) = \int_0^1 I_g(s)\, dg = \int_0^1 \left\{ [a(T_w, g) I_{bw}] e^{-kX(0,s)} + \int_0^s [a(T(s'), g) I_b(s')] e^{-kX(s',s)} k\, u(s')\, ds' \right\} dg. \quad (17)$$

Comparing with equation (7) we find that I_g satisfies the general RTE, equation (1), subject to the same boundary conditions, but for a spectrally-integrated, gray case with the Planck function replaced by a weighted value, $[a I_b]$:

$$\frac{dI_g}{ds} = k(g) u(s) \left([a I_b] - I_g \right), \quad 0 \le g \le 1. \quad (18)$$

What remains to be done is to solve the gray medium RTE, equation (18), by any arbitrary solution method for a small number of gray absorption coefficients $k(g)$ (since k is a smooth, monotonic function in g), followed by numerical quadrature over I_g. In the correlated–k approach this is generally done by Gaussian quadrature, since this gives a high degree of accuracy with relatively few RTE evaluations. The most primitive (and least accurate) quadrature scheme would be the use of the trapezoidal rule; i.e.,

$$\int_0^1 I_g\, dg \simeq \sum_{i=1}^{n} I_g\,(k\,(g_i))\, \Delta g_i; \quad \sum_{i=1}^{n} \Delta g_i = 1, \quad (19)$$

which would imply

$$\alpha = 1 - \tau = \int_0^1 a(T, g) \left(1 - e^{-k(g)X} \right) dg \simeq \sum_{i=1}^{n} A_i(T) \left(1 - e^{-k_i X} \right), \quad (20)$$
$$A_i = \int_{\Delta g} a_i dg$$

which is commonly known as the "Weighted-Sum-of-Gray-Gases" (WSGG) method. Therefore, the Weighted-Sum-of-Gray-Gases method, while a very powerful method in itself, is effectively only a crude implementation of the Full-Spectrum correlated–k approach presented here. Nevertheless, the WSGG method as presented in equation (**??**) is a considerable improvement over the previous state-of-the-art, which allows only cumbersome and inaccurate application to inhomogeneous media [2, 6, 7].

Note that expressing the transmissivity in terms of the correlated–k distribution $f(T, k)$ [second formulation in equation (13)] also satisfies the RTE, replacing the $[a I_b]$ in equation (18) by $[f(T, k) I_b]$, in which case the resulting intensity has to be integrated over k–space, i.e., $I = \int_0^\infty I_k dk$ [10]. The advantage of the present formulation – besides demonstrating the equivalence between k–distribution and the WSGG model – is the fact that the weight function $a(T, g)$ is much smoother and better behaved than the k–distribution, and this requires fewer quadrature points (i.e., gray–gas evaluations) for the accurate determination of full spectrum results such as heat flux.

The validity of the Full-Spectrum correlated–k distribution /Weighted-Sum-of-Gray-Gases model was derived here for a black enclosure with a non-scattering medium. However, it is well known that k–distributions also hold in the presence of gray walls and/or gray scattering particles. This can be shown to be true here by applying the reordering method of equation (13) directly to the full RTE (including scattering), or through physical arguments following the Weighted-Sum-of-Gray-Gases approach: In equation (13) it is stated that — for a straight path — the spectral transmissivity is the same for all spectral positions, which have the same value of k_η. It is immediately obvious that this statement also holds true for any (non-straight) path including any number of (gray) wall reflections and particle scattering events.

It remains to determine the $k(T, g)$ distributions for a given gas mixture followed by transformation to $k(T_0, g_0)$, i.e., the evaluation of the $a(T, g_0)$. This can be done in a number of ways, the two most extreme ones being calculation from (i) total emissivity (transmissivity) data, and (ii) from line-by-line data such as the HITRAN database [20]. HITRAN92 has been used successfully in meteorological applications, but is known to be inaccurate for combustion scenarios since many hot lines are missing in that database. HITRAN96 has remedied this problem to some extent and may now be used with confidence for up to 1000K, although many hot lines are still missing. Very recently, HITEMP has become available for carbon dioxide and water vapor and should be accurate for all combustion level temperatures. However, it has many times the number of spectral lines than HITRAN96, requiring substantically more computer time, and is limited to carbon dioxide and water vapor mixtures. In either case $k(T, g)$ is determined from equation (13) for a fixed reference condition [the same one used in equation (5) with X being some appropriate

length variable such as $p_a L$, where p_a is the partial pressure of the absorbing gas, and L is the geometric length of the gas column]. Recall that the temperature dependence in $k(T, g)$ originates from the fractional Planck function i in equation (13), *not* from the absorption coefficient, which is evaluated at the reference condition (which remains fixed). The transformation function $a(T, g_0)$ is then determined from equation (15) by ratioing values of $f(T, k)$ and $f(T_0, k)$ at identical values of *k*. Alternatively one may ratio the slopes of the g distribution functions for the actual and the reference temperature for the same *k*. Once the correlated–*k* distribution and the weight function have been determined, the temperature and additional pressure dependence given by the function $u(T, p,$concentration) in equation (5) must be postulated and/or determined by fitting equation (13) to total transmissivity values.

If $k(g)$ is to be determined from total emissivity data or correlations, such as the one by Leckner [21], the *k*–distribution $f(k)$ is determined first, since it is simply the inverse Laplace transform of τ. This was first realized by Domoto [22] who found narrowband *k*–distributions from transmissivities obtained from Malkmus' model. The *k*–distribution is then integrated and inverted to yield $k(g)$:

$$f(T,k) = \mathcal{L}^{-1}(\tau(X));$$
$$g(k) = \int_0^k f\,dk = \int_0^k \mathcal{L}^{-1}(\tau(X))dk, \quad \Rightarrow \quad k(T,g). \qquad (21)$$

There are several different ways to obtain $k(T, g)$ from line-by-line data as described in several papers [14–16, 23]. We prefer the following method, which is simple, quick, adaptive and particularly well-suited for full-spectrum calculations: the spectrum $0 \le \eta \le \infty$ is subdivided into N equal subintervals, and $N + 1$ equally spaced spectral locations. Similarly, the *k*–range is subdivided into J ranges (because of the large fluctuation in absorption coefficient, the *k*–range is subdivided equally on a $\log_{10} k$–basis). A set of temperatures T_i can be considered simultaneously. A scan is now made over the $N+1$ spectral locations, the local value of *k* is calculated, and the j-th *k*–bin for the i-th temperature T_i is incremented by the corresponding fractional Planck function if $k_j \le k < k_{j+1}$, i.e., $I_{b\eta}\delta\eta$, with a resolution fine enough that $I_{b\eta}(T_i)$ is constant across $\delta\eta$. At the end of the scan all bin values are multiplied by $\pi/\sigma T_i^4$, after which they reflect the calculated values for $f(T, k_j)$ and the cumulative *k*–distribution for each temperature follows from

$$g(T,k_j) = \sum_{j'=1}^{j} f(T,k_{j'}) = g(T,k_{j-1}) + f(T,k_j) \qquad (22)$$

Note that the number of *k*–bins as well as temperature bins can be made arbitrarily large without any appreciable increase in computation time. While that may result in empty bins, the $g(T, k)$ distribution would simply remain constant for adjacent j-values. After each scan the number of N is doubled, resulting in N additional knot points, and N additional *k*–values are calculated and placed in the $f(T, k_j)$ bins, until such time when the g_j no longer change beyond some criterion. This method also allows an efficient calculation of the transformation function $a(T, g_0)$: since from equation (15), we find that

$$a(T,k_j) = \frac{f(T,k_j)}{f(T_0,k_j)} \qquad (23)$$

and the corresponding g_0 is found from equation (22) as $g(T_0, k_j)$.

SAMPLE CALCULATIONS

The validity of the present model, its application to non–black walls and scattering media, and its limitations due to the scaling approximation will be shown through a number of relatively simple one-dimensional examples in which CO_2–N_2 mixtures confined between two infinite parallel walls are considered. Easily extended to two or three dimensions, the one–dimensional geometry was chosen to test the model. In most of the examples, the P–1 approximation is employed since it is a very popular method with reasonable levels of effort and accuracy together with the Full-Spectrum Correlated–*k* distribution approach. The HITRAN96 database [20] is used in the following calculation to validate the new approach, to limit the amount of CPU time required for line-by-line calculations. For actual heat transfer calculations at these temperature levels the use of the HITEMP database, with its additional hot lines, would be expected to yield more accurate results.

First an isothermal medium confined between two parallel, cold and black plates is considered. The medium is a nitrogen-carbon dioxide mixture at 1500K, 1bar, with a 10% mole fraction of CO_2. Using the HITRAN96 database for the evaluation of absorption coefficients, benchmark line-by-line results are compared in Fig. 2 with our Full-Spectrum Correlated–*k* (FSCK) method for two slab widths demonstrating that the FSCK method is indeed exact for homogeneous media. Using 10 Gaussian quadrature points, the FSCK results essentially coincide with the LBL results (for which approximately 600,000 quadrature points were needed). Using only 6 quadrature points shows slight discrepencies for optically thick cases (L=1m).

Taine et al. [19] have shown that the scaling approximation may produce substantial errors when radiation emitted in a hot region travels through a cold layer, since (i) *k*–distributions always sort absorption coefficients according to magnitude (assuming that this produces consistent wavenumber sorting), while

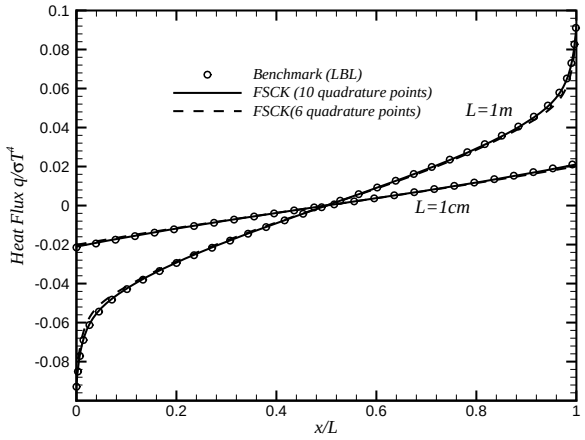

Figure 2. Local radiative flux in an isothermal N_2–CO_2 mixture (T=1500K, p=1bar, y_{CO_2}=0.1, L=1cm and L=1m) bounded by cold, black walls

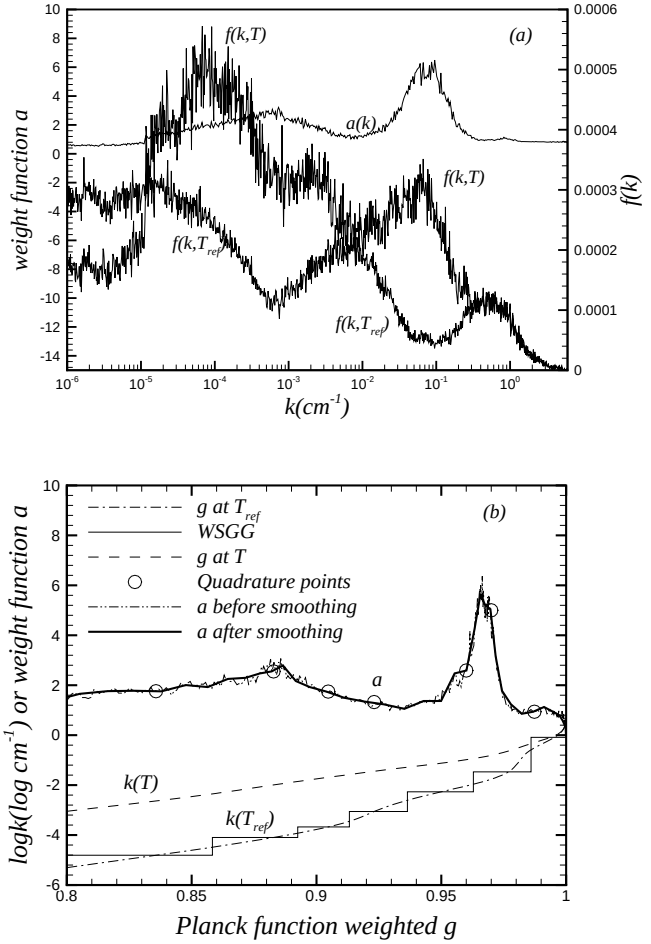

Figure 3. (a) Comparison of *k*–distributions at different temperatures and the weight function a, (b) Planck function weighted cumulative *k*–distribution g, and the weight function a

(ii) in strongly non–isothermal media this ordering consistency is violated by "hot lines," which have large absorption coefficients at high temperature, while being essentially negligible at low temperatures. This causes the scaling approximation to always underpredict the transmissivity of a cold layer adjacent to a hot layer. Therefore, we will consider two types of non-isothermal media. First, we will look at the extreme case of an isothermal hot layer adjacent to an isothermal cold layer. This extreme test will allow us to find out optimum ways to determine accurately scaled absorption coefficient distributions from the HITRAN96 database. This will be followed by a more benign example of a parabolic temperature distribution, which can demonstrate the accuracy of the FSCK method in more typical applications. The FSCK calculations required 10 secconds (10 quadrature points) on an SGI 0200 (single processor R10000 150MHz), while the LBL calculations required 8-10 CPU hours. LBL calculations would be still more costly, if the new HITEMP database (with its many more lines) were used.

By making a transformation from $f(k)dk$ to the weight function $a(T,g)dg$ it was hoped to obtain a smoothened function for easier quadrature [similar to the transformation from $f(k)dk$ to dg, with *k*(g) being a much smoother function than $f(k)$]. This is demonstrated for the case of CO_2 in Fig. 3(a) for two extreme temperatures, T_{hot}=1500K and T_{cold}=500K, showing $f(T_{\text{cold}},k)$, $f(T_{\text{hot}},k)$ and $a(T_{\text{cold}},k)$=$f(T_{\text{cold}},k)/f(T_{\text{hot}},k)$, using the hot gas temperature as the reference state. The corresponding *k*(T,g), together with $a(T,g)$ are shown in Fig. 3(b). While the weight function $a(T,g)$ is not as smooth as the *k*(T,g) function, a is considerably better behaved than the $f(T,k)$: high frequency oscillations are reduced from approximately 25% of maximum to about 5%. Low frequency oscillations are also much less severe. As the temperature moves closer to the reference value, a becomes pregressively smoother (hovering around an average value of a = 1). Therefore, accurate numerical quadrature of equation (19) becomes relatively easy. Note that, in the ADF method [9], the $[aI_b]$ term in equation (18) is replaced by $f(T,k)I_b(T)$, which is much more poorly behaved, making quadrature over all possible *k* values considerably more difficult. Efficient quadrature can be further improved by smoothing the weight function through

$$\int_0^1 a(g)\phi\left(k(g)\right)dg = \int_0^1 \frac{1}{\Delta g}\int_{\Delta g} a(g')\phi(k(g'))dg'\,dg$$

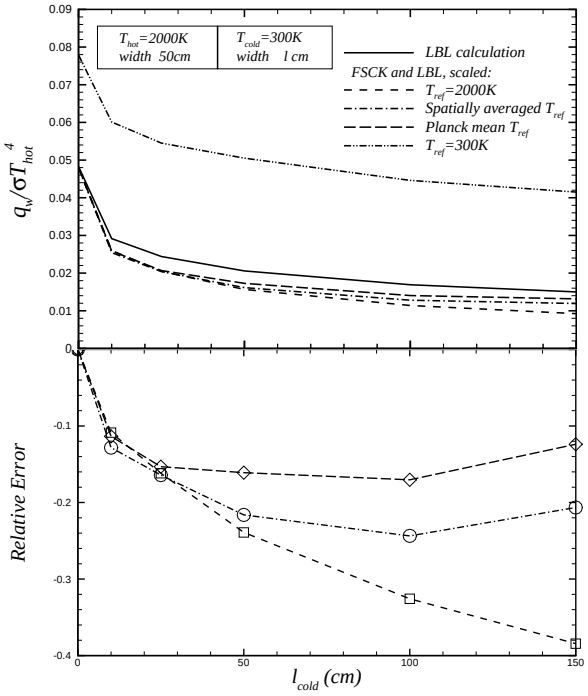

Figure 4. Radiative flux exiting from the cold column of a two-column CO_2–nitrogen mixture at different temperatures (T_{hot}=2000K, l_{hot}=50cm; T_{cold}=300K, l_{cold} variable) and their relative errors; uniform p=1bar, y_{CO_2}=0.1, cold, black wall at T=300K.

$$\simeq \int_0^1 \overline{a}(g)\phi(k(g))dg \tag{24}$$

where,

$$\overline{a} = \frac{1}{\Delta g}\int_{\Delta g} a(g')dg' \tag{25}$$

since $k(g)$ is essentially constant across a small interval Δg. In this expression $\phi(k)$ is any function that depends on g through the function $k(T, g)$, such as I_g. The smoothened weight function $\overline{a}$ is also indicated in Fig. 3(b) along with typical quadrature points used in later examples. Also indicated are typical step values k_i for the WSGG trapezoidal integration.

Figure 4 shows the radiative heat flux arriving at the cold black wall of a N_2–CO_2 mixture with a step in temperature. Pressure and CO_2 mole fraction are constant throughout at 1bar and 10% respectively. The hot layer is at T=2000K and has a fixed width of 50cm, while the cold layer is at 300K, and is of varying width. The LBL results obtained from the HITRAN96 database are compared with various scaling approximations. For the FSCK calculations 20 quadrature points were used, which assured that these results were identical to corresponding LBL results that used the same scaled absorption coefficent (not shown). Determining a scaled absorption coefficient distribution consists of two steps. First, a reference temperature must be chosen, at which the absorption coefficient is set to coincide with that of the database, i.e., the $k_\eta(\eta)$ in equation (5). If we neglect pressure effects on the line half widths b_j (generally a good approximation for systems with roughly constant total pressure), then spectral lines become temperature and pressure dependent through only the line intensities S_j. For a pressure based absorption coefficient, the S_j are directly proportional to partial pressure of the CO_2, and the temperature dependence is approximately [16],

$$S_i = S_{i0}\frac{V_0 R_0}{V R}\exp\left[\frac{hc}{k}E''(\frac{1}{T_0}-\frac{1}{T})\right] \tag{26}$$

where E'' is the energy of the lower state of the transition. The temperature dependence of the vibrational partition function V/V_0 is close to unity, and that of the rotational partition function R/R_0 is $(T/T_0)^j$, with j equal to 1.0 or 1.5. In actuality, values for E'' vary widely (for CO_2, HITRAN96 lists values for E'' between 0 and 4790cm^{-1}, with many lines with even larger E'' known to be missing). In the scaling approximation we must replace all individual E'' by a single representative value. Since radiative heat fluxes are governed by transmission rates, we evaluate a representative E'' in this research from the implicit relation

$$\int_0^\infty I_{b\eta}(T_{\text{ref}})\exp[-\kappa_\eta(T, p_{CO_2})L_m]d\eta = \int_0^\infty I_{b\eta}(T_{\text{ref}})\exp[-k_\eta u(T, p_{CO_2}, E'')L_m]d\eta \tag{27}$$

where k_η=$\kappa_\eta(T_{\text{ref}}, p$ = 1bar, p_{CO_2} = $p_{CO_2,\text{ref}})$ and $u(T_{\text{ref}}, p_{CO_2,\text{ref}})$ is taken to be equal to 1, while L_m is the mean beam length of the volume under consideration [L_m=1.76(l_{hot}+l_{cold}) for the one-dimensional slab considered here] [12].

It remains to choose an appropriate value for the reference temperature, T_{ref}. Using the high temperature (T_{ref}=2000K here) ensures correct prediction of emission from the hot layer but, since scaling incorrectly assumes strong absorption of hot line emission in the cold layer, heat fluxes to the cold wall are underpredicted by as much as 40% (see Fig. 4). On the other hand, if scaling is based on the low temperature (T_{ref}=300K here), this leads to strong overprediction of emission from the hot medium and, thus, heat flux to the cold wall is always overpredicted. [Replacing equation (25) by a condition that matches total emission

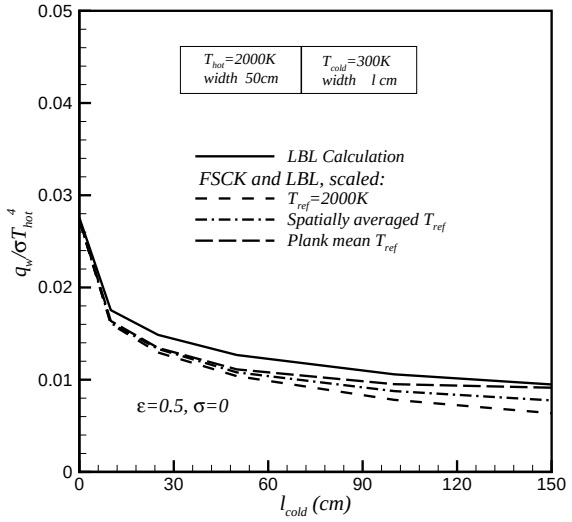

Figure 5. Same as Fig. 4, but for a gray wall with ϵ=0.5

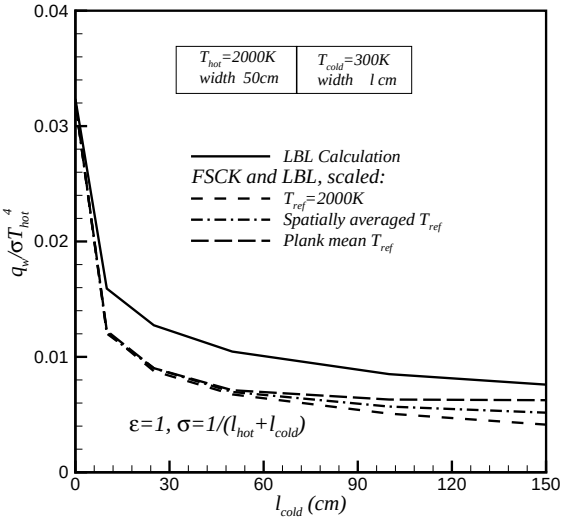

Figure 6. Same as Fig. 4, but with isotropic scattering σ_s=1/($l_{\rm hot}$+$l_{\rm cold}$).

levels also fails, since it cannot correctly predict self-absorption of nearly opaque lines in the hot layer.] Best results were obtained with volumetric average temperatures. A simple volumetric average of T^4, i.e.,

$$T_{\rm ref}^4 = \frac{1}{V}\int_V T^4 dV \tag{28}$$

gives reasonable results, with a maximum error of about 24%. Since equation (28) does not take into account differences between spectral bands and windows, even better results are obtained if a total emission reference temperature is found from the implicit relation involving the Planck-mean absorption coefficient,

$$(\kappa_P T^4)_{\rm ref} = \frac{1}{V}\int_V \kappa_P T^4 dV \tag{29}$$

This choice of $T_{\rm ref}$ reduces the maximum error to about 18% and is, therefore, recommended for general use.

Denison and Webb [4] have already shown that the WSGG method is applicable to gray boundaries. To demonstrate that the FSCK method and, therefore, also the WSGG method is equally valid not only for media bounded by gray walls, but also for (gray) scattering media, heat fluxes through the mixture

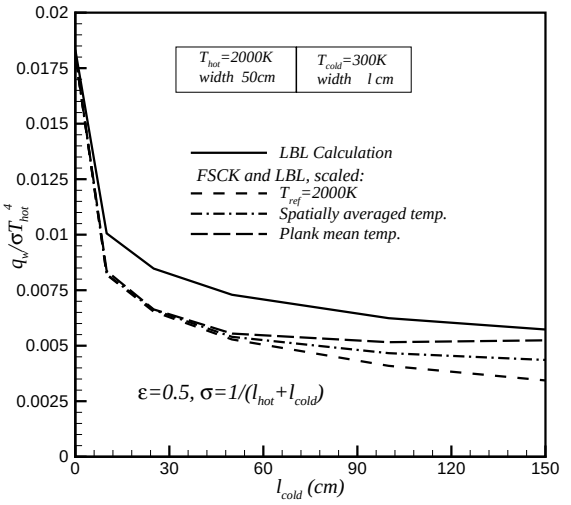

Figure 7. Same as Fig. 4, but with isotropic scattering σ_s=1/($l_{\rm hot}$+$l_{\rm cold}$) and a gray wall with ϵ=0.5.

of the previous example were also calculated for the cases of gray walls (ϵ=0.5), the addition of a gray scattering medium [scattering coefficient σ_s=1/($l_{\rm hot}$+$l_{\rm cold}$)], and the combination of both. Representative calculations using line-by-line calculations together with the scaled absorption coefficient confirmed that the FSCK method produces exact results (for the scaled absorption

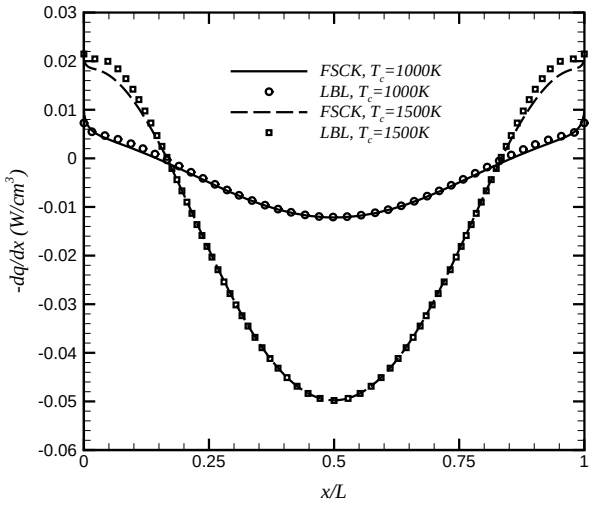

Figure 8. Radiative source in a L=1m thick CO_2–N_2 mixture with parabolic temperature profile and homogeneous concentration [T=T_c−($T_c - T_w$)($2x/L - 1$)^2, T_w=500K, y_{CO_2}=0.1].

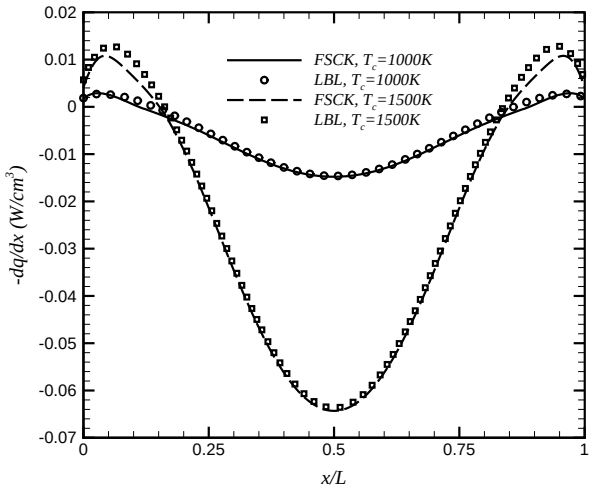

Figure 9. Radiative source in a L=1m thick CO_2–N_2 mixture with parabolic temperature and concentration profiles [T=T_c-($T_c - T_w$)($2x/L$-1)^2, y_{CO_2}=y_c-(y_c-y_w)($2x/L$-1)^2, T_w=500K, y_c=0.2, y_w=0.01.]

coefficient), even in the presence of non-black walls and gray scattering. In all cases using the Planck-mean temperature as the reference value gave again the most accurate results. Inspection of Fig. 5 shows that with the presence of a nonblack wall the heat flux to the wall is reduced and the maximum relative error remains approximately the same. The influence of scattering is shown in Fig. 6 and combined effects in Fig. 7. Qualitatively, the trends remain the same. However, discrepencies between scaled and unscaled absorption coefficients are increased somewhat, with maximum errors at l_{cold}=50cm of 35% (Fig. 6) and 25% (Fig. 7), respectively.

The previous examples with a step change in temperature were designed to be a worst-case scenario, i.e., to understand the limits of the scaling approximation. As a last example we will consider nitrogen-carbon dioxide mixtures with smoothly-varying temperature and/or concentration profiles, such as one may expect to occur in actual combustion applications. Figure 8 shows the radiative source term, $-dq/dx$, in a 1m thick gas layer with a parabolic temperature profile, but constant concentration (p=1bar, y_{CO_2}=0.1). Two different centerline temperatures are considered (1000K and 1500K), while the black wall is kept at 500K in both cases. To obtain a scaled absorption coefficient for the FSCK method, the Planck-mean temperature was used for reference as recommended above. As seen from the figure the LBL and FSCK results virtually coincide. Only for T_c=1500K is there a slight discrepency near the wall (5% of maximum), which is due in part to (i) the limitations of the scaling approximation, and (ii) the fact that a limited number of quadrature points was used in the FSCK method to approximate integration over g with the weight function a. The agreement between LBL and scaled FSCK results is even better (3%) if a parabolic concentration profile is considered (other conditions remaining the same), as shown in Fig. 9.

SUMMARY AND CONCLUSIONS

A Full-Spectrum correlated–*k* distribution (FSCK) has been developed, which–within its limitations (gray walls, gray scattering, spectral absorption coefficient obeying the scaling approximation) — allows very efficient "exact" evaluation of radiative fluxes for arbitrary molecular gas mixtures, using any desired RTE solver. It has been shown that the popular Weighted-Sum-of-Gray-Gases (WSGG) method is simply a crude implementation of the FSCK method; therefore, it is implied that the WSGG method can also be applied to gray enclosures as well as gray scattering media. Limitations of the scaling approximation have also been investigated and procedures to find optimally scaled distributions have been discussed.

ACKNOWLEDGMENTS

The authors gratefully acknowledge the financial support of the National Science Foundation under the contract CTS-9615009.

REFERENCES

[1] Hottel, H. C. and Sarofim, A. F., 1967, *Radiative Transfer*, McGraw-Hill, New York.

[2] Modest, M. F., 1991, "The Weighted-Sum-of-Gray-Gases Model for Arbitrary Solution Methods in Radiative Transfer", *ASME Journal of Heat Transfer*, **113**(3), pp. 650–656.

[3] Denison, M. K and Webb, B. W., 1993, "An Absorption-Line Blackbody Distribution Function for Efficient Calculation of Total Gas Radiative Transfer", *Journal of Quantitative Spectroscopy and Radiative Transfer*, **50**, pp. 499–510.

[4] Denison, M. K and Webb, B. W., 1993, "A Spectral Line Based Weighted-Sum-og-Gray-gases Model for Arbitrary RTE Solvers", *ASME Journal of Heat Transfer*, **115**, pp. 1004–1012.

[5] Denison, M. K. and Webb, B. W., 1994, "k-Distributions and Weighted-Sum-of-Gray Gases: A Hybrid Model", In *Tenth International Heat Transfer Conference*, Taylor & Francis, pp. 19–24.

[6] Denison, M. K. and Webb, B. W., 1995, "The Spectral-Line-Based Weighted-Sum-of-Gray-Gases Model in Nonisothermal Nonhomogeneous Media", *ASME Journal of Heat Transfer*, **117**, pp. 359–365.

[7] Denison, M. K. and Webb, B. W., 1995, "Development and Application of an Absorption Line Blackbody Distribution Function for CO_2", *International Journal of Heat and Mass Transfer*, **38**, pp. 1813–1821.

[8] Denison, M. K. and Webb, B. W., 1995, "The Spectral-Line Weighted-Sum-of-Gray-Gases Model for H_2O/CO_2 Mixtures", *ASME Journal of Heat Transfer*, **117**, pp. 788–792.

[9] Rivière, Ph., Soufiani, A., Perrin, Y., Riad, H., and Gleizes, A., 1996, "Air Mixture Radiative Property Modelling in the Temperature Range 10000-40000 K", *Journal of Quantitative Spectroscopy and Radiative Transfer*, **56**, pp. 29–45.

[10] Pierrot, L., Rivière, Ph, Soufiani, A., and Taine, J., 1999, "A Fictitious-gas-based Absorption Distribution Function Global Model for Radiative Transfer in Hot Gases", *Journal of Quantitative Spectroscopy and Radiative Transfer*, **62**, pp. 609–624.

[11] Pierrot, L., Soufiani, A., and Taine, J., 1999, "Accuracy of Narrow-band and Global Models for Radiative Transfer in H_2O, CO_2, and H_2O-CO_2 Mixtures at High Temperature", *Journal of Quantitative Spectroscopy and Radiative Transfer*, **62**, pp. 523–548.

[12] Modest, M. F., 1993, *Radiative Heat Transfer*, McGraw-Hill, New York.

[13] Goody, R. M. and Yung, Y. L., 1989, *Atmospheric Radiation - Theoretical Basis*, Oxford University Press, New York, 2nd ed.

[14] Goody, R., West, R., Chen, L., and Crisp, D., 1989, "The Correlated k Method for Radiation Calculations in Nonhomogeneous Atmospheres", *Journal of Quantitative Spectroscopy and Radiative Transfer*, **42**, pp. 539–550.

[15] Fu, Q. and Liou, K. N., 1992, "On the Correlated k-Distribution Method for Radiative Transfer in Nonhomogeneous Atmospheres", *Journal of the Atmospheric Sciences*, **49**(22), pp. 2139–2156.

[16] A., Lacis A. and Oinas, V., 1991, "A Description of the Correlated-k Distribution Method for Modeling Nongray Gaseous Absorption, Thermal Emission and Multiple Scattering in Vertically Inhomogeneous Atmospheres", *J. of Geophysical Research*, **96**.

[17] Rivière, Ph., Soufiani, A., and Taine, J., 1992, "Correlated-k and Fictitious Gas Methods for H_2O near 2.7 μm", *Journal of Quantitative Spectroscopy and Radiative Transfer*, **48**, pp. 187–203.

[18] Rivière, Ph., Soufiani, A., and Taine, J., 1995, "Correlated-K and fictitious gas model for H_2O infrared radiation in the Voigt regime", *Journal of Quantitative Spectroscopy and Radiative Transfer*, **53**, pp. 335–346.

[19] Taine, J. and Soufiani, A., 1999, *Gas IR Radiative Properties: From Spectroscopic Data to Approximate Models*, **33**, Academic Press, New York.

[20] Rothman, L. S., Rinsland, C. P., Goldman, A., Massie, S. T., Edwards, D. P., Flaud, J. M., Perrin, A., Camy-Peyret, C., Dana, V., Mandin, J. Y., Schroeder, J., McCann, A., Gamache, R. R., Wattson, R. B., Yoshino, K., Chance, K. V., Jucks, K. W., Brown, L. R., Nemtchinov, V., and Varanasi, P., 1998, "The HITRAN Molecular Spectroscopic Database and HAWKS (HITRAN Atmospheric Workstation): 1996 Edition", *Journal of Quantitative Spectroscopy and Radiative Transfer*, **60**, pp. 665–710.

[21] Leckner, B., 1972, "Spectral and Total Emissivity of Water Vapor and Carbon Dioxide", *Combustion and Flame*, **19**, pp. 33–48.

[22] Domoto, G. A., 1974, "Frequency Integration for Radiative Transfer Problems Involving Homogeneous Non-gray Gases: The Inverse Transmission Function", *Journal of Quantitative Spectroscopy and Radiative Transfer*, **14**, pp. 935–942.

[23] Arking, A. and Grossman, K., 1972, "The Influence of Line Shape and Band Structure on Temperatures in Planetary Atmospheres", *Journal of the Atmospheric Sciences*, **29**, pp. 937–949.